

A Hybrid and Efficient Adaptive Cartesian Grid for Simulation of Unsteady Flow in Aerodynamics Applications

Mir Yoseph Hashemi¹

Alireza Jahangirian²

Nima Molani³

Abstract — A Hybrid Grid Generation Method that combines the computational efficiency of the Cartesian grid and the flexibility of the meshless strategy is developed for computation of the compressible inviscid flows over general geometries and moving boundary applications. The meshless zone is created around the geometry by producing layers of nodes along normal direction vectors while Cartesian grid method is used elsewhere. Last layer is used as virtual geometry for automatic generation of unstructured Cartesian grid around meshless zone. An efficient central difference scheme with artificial dissipation terms is developed for both Cartesian grid and meshless zones. The method is used for computation of flows around stationary, moving and oscillating airfoil at subsonic and transonic flow conditions. Results indicate good agreements with other reference numerical data.

Keywords: Adaptive Cartesian Grid, Moving Boundary, MeshLess Method

I. Introduction

The main problem of Computational Fluid Dynamics (CFD) is mesh generation for configurations with complex geometry specially with moving boundaries. The structured grid methods are not efficient for such cases. The main advantage of unstructured grid methods is the facility of grid generation for complex configurations. However, the computational costs and memory requirements are generally higher than their structured grid counterparts. Alternatively, the unstructured Cartesian grid methods can be used that offer ease of grid generation, lower computational storage requirements, and significantly less operational count per cell compared to body fitted curvilinear grids [1]. Embedded and adaptive grids, can also be used to provide better resolution and moving of geometry and flow features in Cartesian grid. However, the main challenge in using this method deals with arbitrary boundaries. As the grids are not body aligned, Cartesian cells near the body can extend through surfaces of solid components. Hence, accurate means of representations for surface boundary conditions are essential for the success of Cartesian schemes.

¹ Mir Yuseph Hashemi
Azarbaijan Shahid Madani University
Iran

²Alireza Jahangirian
Amirkabir University of Technology
Iran

³ Nima Molani
Istanbul Technical University
Turkey

In this research a hybrid grid generation method that combines the computational efficiency of the Cartesian grid and the flexibility of the meshless strategy is developed for computation of the compressible viscous flows over general geometries and moving boundary applications. The meshless zone is created around the geometry by producing layers of nodes along normal direction vectors while Cartesian grid method is used elsewhere. Last layer is used as virtual geometry for automatic generation of unstructured Cartesian grid around meshless zone. Since the majority of computational domain is solved using the Cartesian grid method, the resulting procedure is very efficient in terms of both computational cost and storage requirements. In addition, since the meshless method is used to obtain the solution for the solid boundary points the developed method can easily be used for complex geometries without need to generate the body-fitted mesh. The Cartesian grid is then adapted to

the location of virtual geometries and flow solution to enhance the quality of the results with the minimum computational cost. The Navier-Stokes equations are solved using a cell-centered finite volume scheme in Cartesian grid zone with second order central difference that stabilized by artificial dissipation [2]. Like finite difference method, the meshless algorithm is applied directly to the differential form of the governing equations. Almost all of meshless methods makes use of a least-square formulation [3]. The least-square discretization is stabilized by artificial dissipation.

The hybrid method was development to moving boundary applications such as moving airfoil at stationary fluid or oscillating airfoil at fluid flows. An advantage of this approach for unsteady moving boundary problems is that the Cartesian grid is fixed similar to a background grid and the meshless zones are moving on top of the Cartesian grid. The Cartesian grid is then adapted to virtual geometry position. Thus the equations of flow are solved in arbitrary Lagrangian–Eulerian formulation in meshless zone and Eulerian formulation in Cartesian grid. The Cartesian grid is adapted to the new virtual geometry and flow solution to enhance the quality of the results with the minimum computational cost. An efficient binary tree data structure is used for generating Cartesian grid. The development dual-time implicit time discretization scheme is then applied to the presented for calculation of compressible inviscid flow on hybrid grid.

II. Governing Flow Equations

Two-dimensional compressible inviscid flow equations consisting of the mass, momentum, and energy conservation

laws. The flow domain is divided to two zones. A first zone is adaptive Cartesian grid that is fixed. The governing equations solve in Eulerian form that can be written in the differential form as:

$$\frac{\partial \mathbf{w}}{\partial t} + \frac{\partial \mathbf{f}_1}{\partial x} + \frac{\partial \mathbf{g}_1}{\partial y} = 0 \quad (1)$$

where

$$\mathbf{w} = \begin{pmatrix} \rho \\ \rho u \\ \rho v \\ \rho E \end{pmatrix}, \mathbf{f}_1 = \begin{pmatrix} \rho u \\ \rho uu + P \\ \rho uv \\ \rho Eu + Pv \end{pmatrix}, \mathbf{g}_1 = \begin{pmatrix} \rho v \\ \rho uv \\ \rho vv + P \\ \rho Ev + Pv \end{pmatrix} \quad (2)$$

Here P , ρ , u , v and E denote the pressure, density, Cartesian velocity components in x and y directions and total energy, respectively. For a perfect gas:

$$P = \rho(\gamma - 1) \left[E - \frac{u^2 + v^2}{2} \right] \quad (3)$$

where γ is the ratio of specific heats.

The second is meshless zone that moves on the first zone. Therefore The governing equations solve in Lagrangian-Eulerian form that can be written in the differential form as:

$$\left[\frac{\partial \mathbf{w}}{\partial t} + \mathbf{w} \nabla \cdot \mathbf{w}_s \right] + \left[\frac{\partial \mathbf{f}_2}{\partial x} + \frac{\partial \mathbf{g}_2}{\partial y} \right] = 0 \quad (4)$$

where

$$\mathbf{w}_s = \begin{pmatrix} x_i \\ y_i \end{pmatrix}, \mathbf{f}_2 = \begin{pmatrix} \rho U \\ \rho uU + P \\ \rho vU \\ \rho EU + Pu \end{pmatrix}, \mathbf{g}_2 = \begin{pmatrix} \rho V \\ \rho uV \\ \rho vV + P \\ \rho EV + Pv \end{pmatrix} \quad (5)$$

where \mathbf{w}_s is vector of point velocity and x_i , y_i are components of velocity in x and y directions, respectively.

III. Numerical Method

A. Finite volume spatial discretization for Cartesian grid

The Euler equations are solved using a central second order cell-centered finite volume scheme in Cartesian grid zone that was stabilized artificial dissipations [2]. The finite volume approximation of the cell k becomes:

$$A_{\Omega_i} \frac{d}{dt} (\mathbf{w}_i) + \mathbf{E}_i(\mathbf{w}) - \mathbf{D}_i(\mathbf{w}) = 0 \quad (6)$$

where A_{Ω_i} is the cell area, $\mathbf{E}_i(\mathbf{w})$ is the convective flux integration for cell i and $\mathbf{D}_i(\mathbf{w})$ is the artificial dissipation terms are given by:

$$\mathbf{D}_i(\mathbf{w}) = \sum_{\ell=1}^n \mathbf{d}_{\ell}^{(2)} + \sum_{\ell=1}^n \mathbf{d}_{\ell}^{(4)}$$

$$\mathbf{d}_{\ell}^{(2)} = \lambda_{\ell} \varepsilon_{\ell}^{(2)} (\mathbf{w}_p - \mathbf{w}_k)_{\ell}, \mathbf{d}_{\ell}^{(4)} = \lambda_{\ell} \varepsilon_{\ell}^{(4)} (\nabla^2 \mathbf{w}_p - \nabla^2 \mathbf{w}_k)_{\ell} \quad (7)$$

$$\lambda_{\ell} = |u_{\ell} \Delta y_{\ell} - v_{\ell} \Delta x_{\ell}| + a_{\ell} \sqrt{\Delta x_{\ell}^2 + \Delta y_{\ell}^2}$$

$$\nabla^2 \mathbf{w}_i = \sum_{\ell=1}^n (\mathbf{w}_p - \mathbf{w}_k)$$

where p and k are the number of cell in right and left of edge ℓ , respectively. u_{ℓ} and v_{ℓ} are the velocity components and a_{ℓ} is the speed of sound on edge ℓ . k_2 and k_4 are two empirically chosen constants, which typically have values in the range $0.5 < k_2 < 1$ and $\frac{1}{256} < k_4 < \frac{1}{32}$. The flow variables on edge ℓ evaluating with arithmetic averaging.

B. Spatial discretization for meshless zone

The least-square meshless method is used to discretization of the flow equations in the conservation form. The spatial derivatives of the function by using the least-square method[4]:

$$\frac{\partial \phi}{\partial x_i} = 2 \sum_{j=1}^m a_{ij} (\phi_{j+1/2} - \phi_i), \frac{\partial \phi}{\partial y_i} = 2 \sum_{j=1}^m b_{ij} (\phi_{j+1/2} - \phi_i) \quad (8)$$

where $j + 1/2$ is the mid-point of the edge ij , where j is in a cloud of point i (Fig.1). The coefficients in Eq. (8) are least-square coefficients and can be calculated using the inverse distance weighting function as:

$$a_{ij} = \frac{\omega_{ij} \Delta x_{ij} \sum_{k=1}^m \omega_{ik} \Delta y_{ik}^2 - \omega_{ij} \Delta y_{ij} \left(\sum_{k=1}^m \omega_{ik} \Delta x_{ik} \Delta y_{ik} \right)}{\sum_{k=1}^m \omega_{ik} \Delta y_{ik}^2 \sum_{k=1}^m \omega_{ik} \Delta x_{ik}^2 - \left(\sum_{k=1}^m \omega_{ik} \Delta x_{ik} \Delta y_{ik} \right)^2},$$

$$b_{ij} = \frac{\omega_{ij} \Delta y_{ij} \sum_{k=1}^m \omega_{ik} \Delta x_{ik}^2 - \omega_{ij} \Delta x_{ij} \left(\sum_{k=1}^m \omega_{ik} \Delta x_{ik} \Delta y_{ik} \right)}{\sum_{k=1}^m \omega_{ik} \Delta y_{ik}^2 \sum_{k=1}^m \omega_{ik} \Delta x_{ik}^2 - \left(\sum_{k=1}^m \omega_{ik} \Delta x_{ik} \Delta y_{ik} \right)^2} \quad (9)$$

$$\Delta x_{ij} = x_j - x_i, \Delta y_{ij} = y_j - y_i$$

Applying the least-square approximations given by Eq. (8) to each component of flux functions in Eq. (4), a semi-discrete form of the Euler equations at point i is obtained:

$$\left[\frac{\partial \mathbf{w}_i}{\partial t} + \mathbf{w}_i \left(\sum_{j=1}^m a_{ij} \Delta x_{i,j} + \sum_{j=1}^m b_{ij} \Delta y_{i,j} \right) \right] + R_i(\mathbf{w}) = 0 \quad (10)$$

$$R_i(\mathbf{w}) = \left[\sum_{j=1}^m a_{ij} \Delta \mathbf{f}_{2ij} + \sum_{j=1}^m b_{ij} \Delta \mathbf{g}_{2ij} \right]$$

If the numerical flux at the mid-point are evaluated using the simple arithmetic averages of conservative variables at the two end points, the resulting of the numerical scheme is equivalent to the central differencing method. It is well known that such discretization lead to unstable schemes, and must be augmented by stabilizing terms. This can be achieved either by adding directly second and forth order damping terms.

$$\frac{\partial \mathbf{w}_i}{\partial t} + \bar{\mathbf{R}}_i(\mathbf{w}) = 0 \quad (11)$$

$$\bar{\mathbf{R}}_i(\mathbf{w}) = \mathbf{w}_i \left(\sum_{j=1}^m a_{ij} \Delta x_{i,j} + \sum_{j=1}^m b_{ij} \Delta y_{i,j} \right) + \mathbf{R}_i(\mathbf{w}) - \mathbf{D}_i(\mathbf{w})$$

Further details of the dissipation terms calculation can be found in refs [4].

iv. Meshless zone point creation

In the first step, the surface must be broken up into elements (edges in 2D and faces in 3D) for full description of a complex geometry. To generate the efficient distribution of points in the meshless zone around the geometry the unit normal vector for all vertices on the geometry are calculated. At the next step, the layers of nodes are produced along the normal lines until a user specified numbers of layers (Fig. 2).

v. Adaptive Cartesian grid generation

Generation of the unstructured cartesian grid is carried out following the work of Jahangirian and Shoraka [2]. To complement the meshless zone for solution of the governing flow equations a series of halo points are added outside the meshless zone that two layers of Cartesian cells are selected and their centers are considered for meshless zone computations. The close view of the generated final grid (including halo points) around a NACA 0012 airfoil is shown in Fig. 3.

One of the advantages of the Cartesian-based grid generation methods is the ease in which the refinement and coarsening is performed by the tree data structure. The use of binary tree, i.e. allows refined cells to be added to the domain by simply creating new sub-branches logically below the refined cell. Cell coarsening will become more important especially when a transient solution is needed because the position of various phenomena may change during transient solution. In the present work, the solution-based grid adaptation is carried out using the following algorithm [3]:

- (1) Start the adaptation process when the selected equation residual is lower than a specified limit.
- (2) Calculate the indicator parameter for all Cartesian cells.
- (3) Mark cells for refining and coarsening.
- (4) Perform coarsening processes on the Cartesian grid.
- (5) Perform refining processes on the Cartesian grid.
- (6) Check the balancing constraint.
- (7) Interpolate flow properties on the new Cartesian cells.
- (8) Return to the flow solution algorithm.

vi. Results

To demonstrate the capabilities of the present method in generating and adapting the Cartesian grid for moving boundary, a rotating of NACA0012 airfoil and modification of grid for new position is shown in Fig. 4. A test case to validation of hybrid method to simulation unsteady flow is moving the NACA0012 airfoil in the stationary air. The

Mach number of airfoil is 0.5. For comparison purpose, this problem is also run in the steady mode with the airfoil is stationary and the air flow has the speed of Mach 0.5. For the simulation of moving airfoil, the grid motion and the pressure contours at different times are shown in Fig. 5. In Fig. 6 the pressure distributions along the airfoil surface from both the steady state and moving airfoil simulation are compared with each other and data from ref. [5].

The other test case is an unsteady transonic flow over NACA0012 pitching airfoil is considered from the AGARD experimental test cases that is called CT5 case [5]. For this case, the periodic motion of the airfoil is defined by the angle of attack as a function of time as;

$$\alpha = \alpha_m + \alpha_0 \sin(\omega t) \quad (12)$$

where α_m is the mean angle of attack, α_0 is the oscillation amplitude, and ω is the angular frequency of the motion which is related to reduced frequency k by $k = \omega c / 2U_\infty$

and U_∞ is the free stream velocity and c is the chord length of the airfoil. The flow conditions of CT5 case are $M = 0.755$, $\alpha_m = 0.016^\circ$, $\alpha_0 = 2.51^\circ$, $k = 0.0814$. In this case a strong shock wave, that develops alternatively on the upper and lower surface of the airfoil.

In this case the Reynolds number is very high with no separation. Therefore can be suitable test for Euler equation solution validation. Instantaneous pressure contour and adapted grid with meshless zone at different phase angle are shown in Fig. 6. A comparison between the present results for pressure distributions over the airfoil by the experimental and numerical data are shown in Fig. 7 for four different phase angle during the cycle. As is seen, the calculated pressure distribution is shown good agreement with experimental and numerical data. The comparison of lift and pitching moment coefficient with experimental data are shown in Fig. 8. As is seen, the numerical results agree with the experimental and reliable numerical data [5,6,7].

References

- [1] M. J. Aftosmis, "Solution Adaptive Cartesian Grid Methods for Aerodynamic Flows with Complex Geometries," Von Karman Institute for Fluid Dynamics, March 1997, Lecture Series 1999.
- [2] A. Jahangirian, and Y. Shoraka, "Adaptive unstructured grid generation for engineering computation of aerodynamic flows," Mathematics and Computers in Simulation, Vol. 78, p: 627–644, 2008.
- [3] A. Jahangirian, and M. Y. Hashemi, "Adaptive Cartesian grid with mesh-less zones for compressible flow calculations," Computers & Fluids, Vol. 54, p: 10–17, 2012.
- [4] Hashemi, Y., and Jahangirian, "A Implicit fully mesh-less method for compressible viscous flow calculations, Journal of Computational and Applied Mathematics. Vol. 235, p: 4687–4700, 2011.
- [5] AGARD Fluid Dynamics Panel, Compendium of Unsteady Aerodynamic Measurements. AGARD, R -702, 1982.
- [6] S. M. Murman, M. J. Aftosmis and M. J. Berger, "Implicit approaches for moving boundaries in a 3-D Cartesian method", 41th AIAA Aerospace Sciences Meeting, Reno, Nevada, January 6-9, 2003.
- [7] D.J. Kirshman, F. Liu, "Flutter prediction by an Euler method on non-moving Cartesian grids with gridless boundary conditions", Computers & Fluids 35:571-586, 2006.



Mir Yoseph Hashemi received a B.S. degree in Aerospace Engineering from Sharif University of Technology, Tehran, Iran, in 2003, his M.S. degree in Aerospace Engineering from Amirkabir University of Technology (AUT), Tehran, Iran, in 2005, and a Ph.D. degree from AUT, in 2010. In 2010, he joined the Department of Mechanical Engineering, Azarbaijan Shahid Madani University, where he is currently Assistant Professor. His research interests include: computational fluid dynamics, grid generation and meshless Methods.

Iran, in 1992, and a Ph.D. degree from Manchester University, England, in 1997. In 1998, he joined the Department of Aerospace Engineering, AUT, where he is currently Associate Professor. His research interests include: computational fluid dynamics, grid generation and meshless Methods.



Nima Molani received a B.S. degree in Mechanical Engineering from Islamic Azad University of Tabriz, Iran in 2009. He is currently a M.S degree student in Aeronautical and Astronautical engineering major in Istanbul Technical University, Turkey. His research interests include: fluid structure interactions.



Alireza Jahangirian received a B.S. degree in Mechanical Engineering from Amirkabir University of Technology (AUT) Tehran, Iran in 1988, his M.S. degree in Mechanical Engineering from Sharif University of Technology, Tehran,

• Figures and drawings

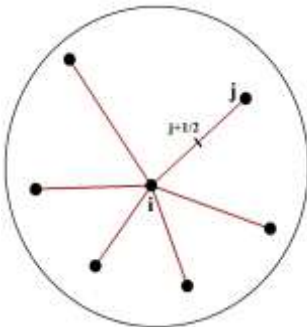


Figure 1. Schematic of point and its neighbors and mid=point.

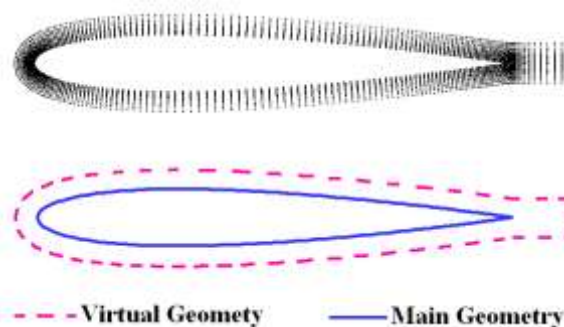


Figure 2. Meshless zone with its outer boundary.

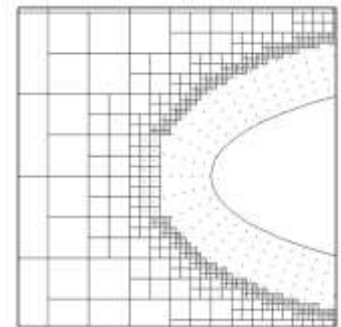


Figure 3. Hybrid Cartesian grid and meshless zones.

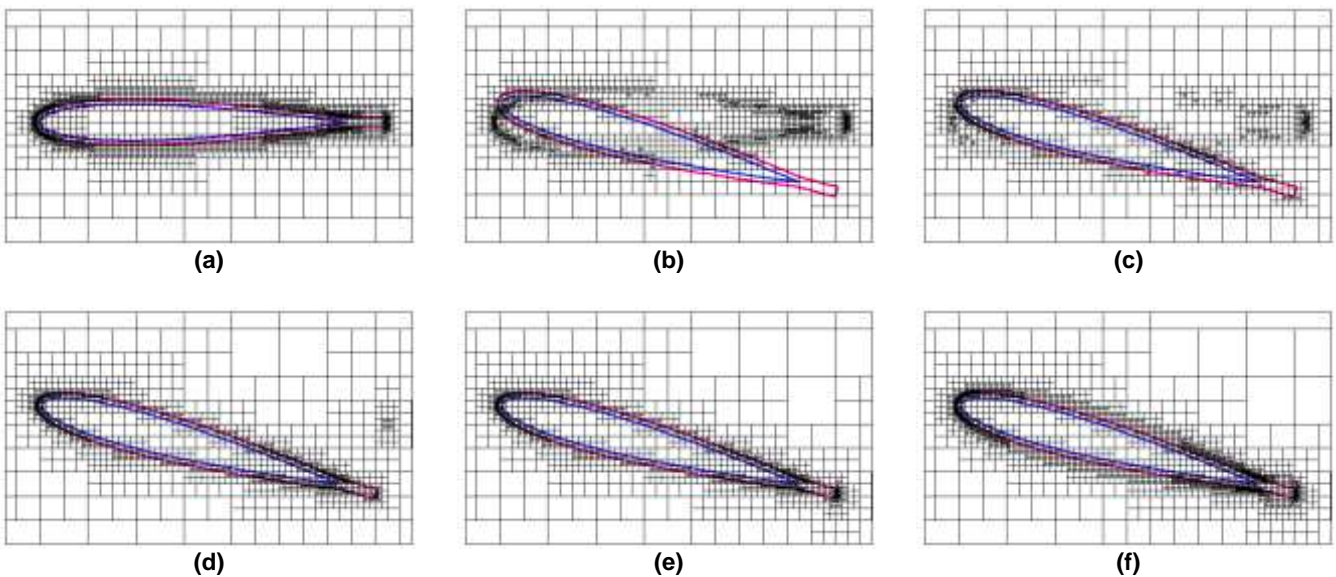


Figure 4. Geometric adaptation of the grid for moving boundaries.

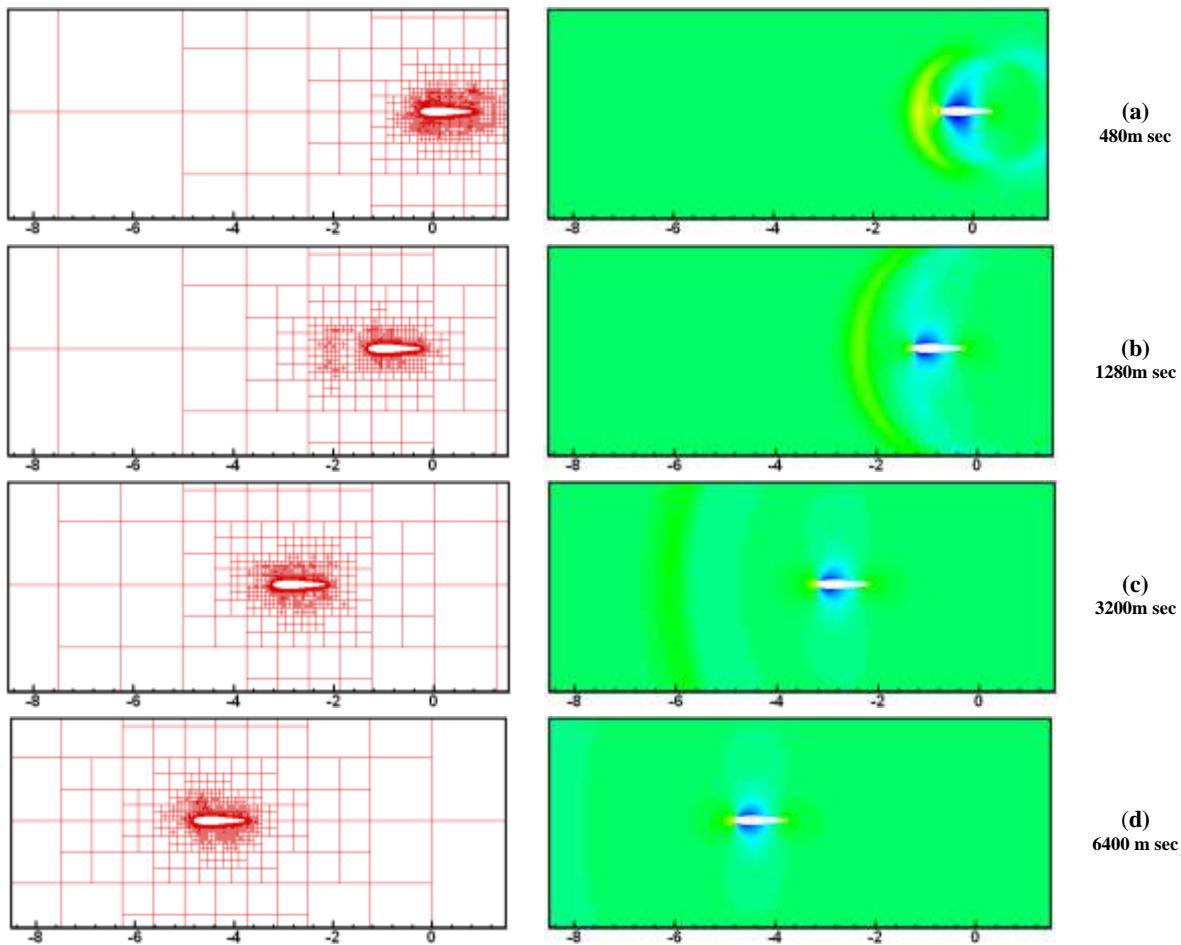


Figure 4. Pressure contours and adapted grid for moving fully Eulerian and fully Lagrangian solution with Mach number 0.5.

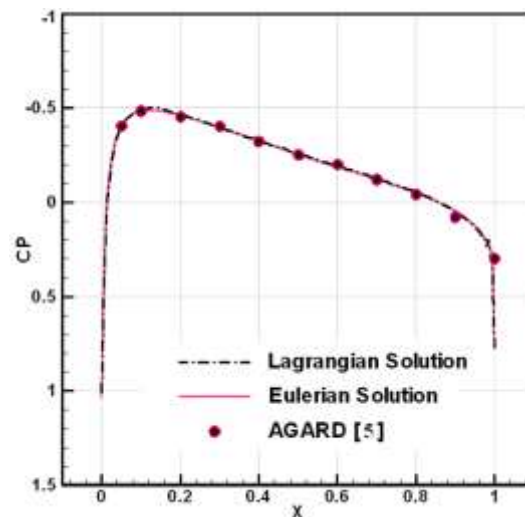


Figure 5. Calculated pressure coefficient distribution over NACA0012 airfoil by fully Eulerian and fully Lagrangian solution with Mach number 0.5.

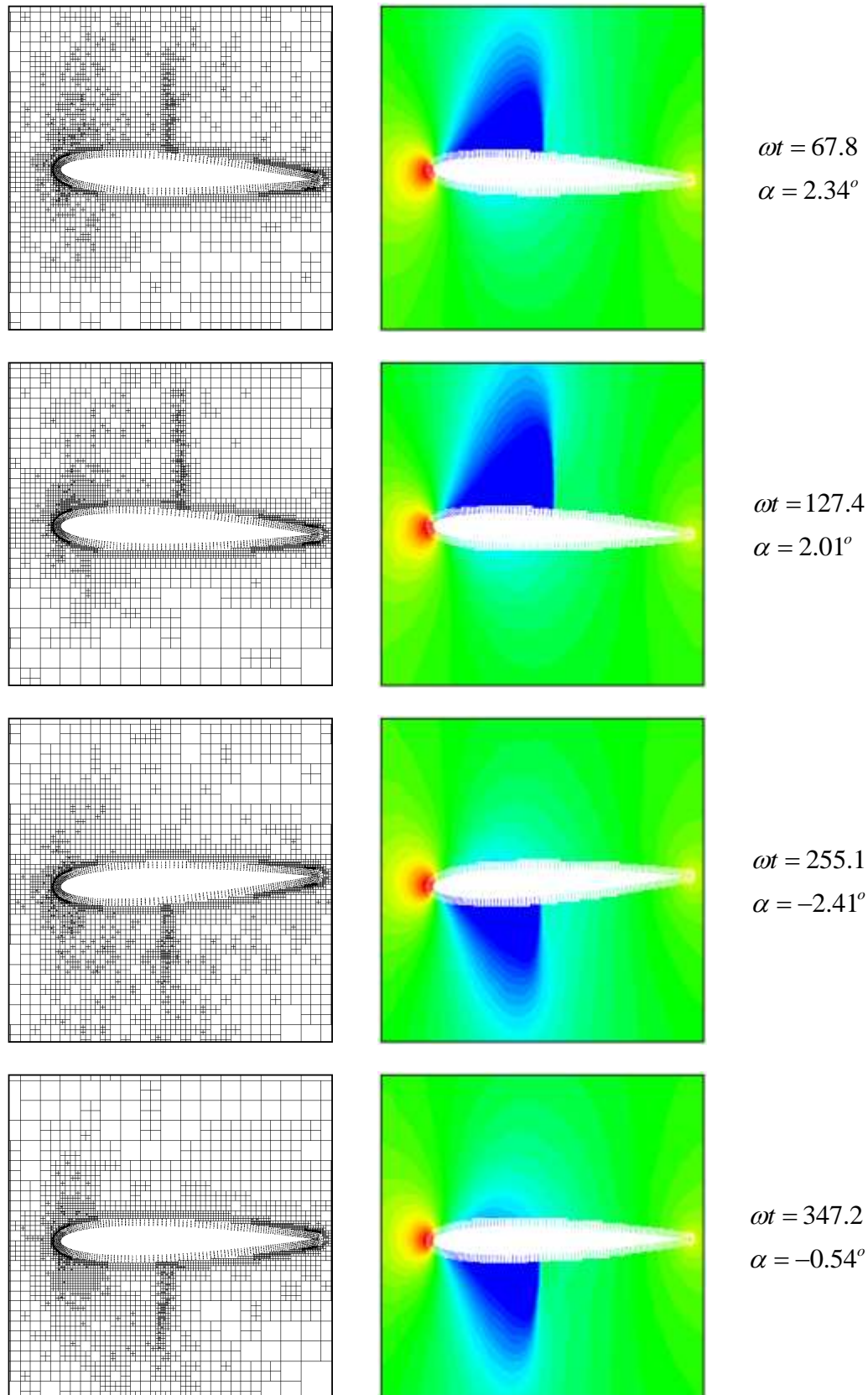


Figure 6. Instantaneous pressure contour and adapted grid with meshless zone for AGARD test case CT5.

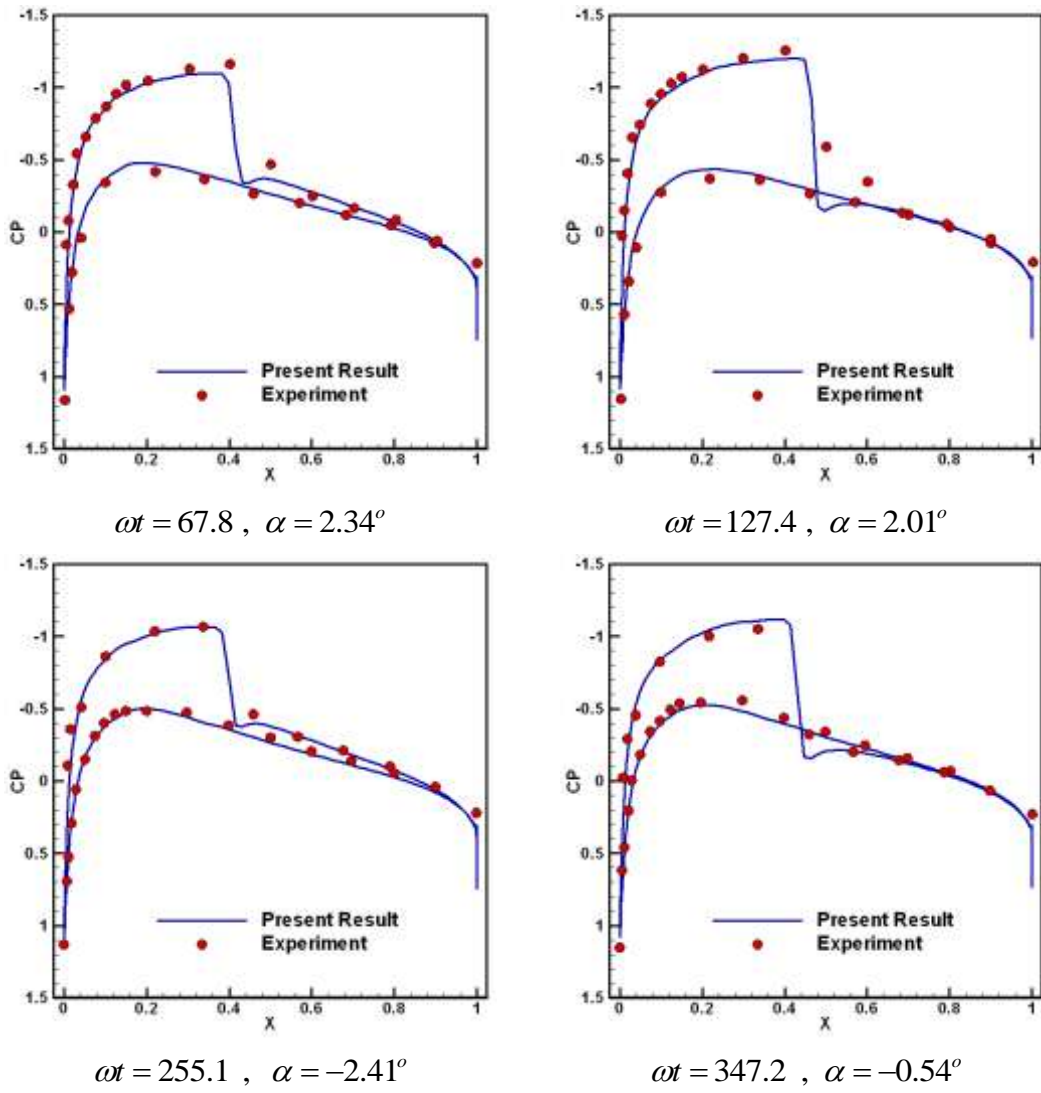


Figure 7. Instantaneous pressure distributions for AGARD test case CT5.

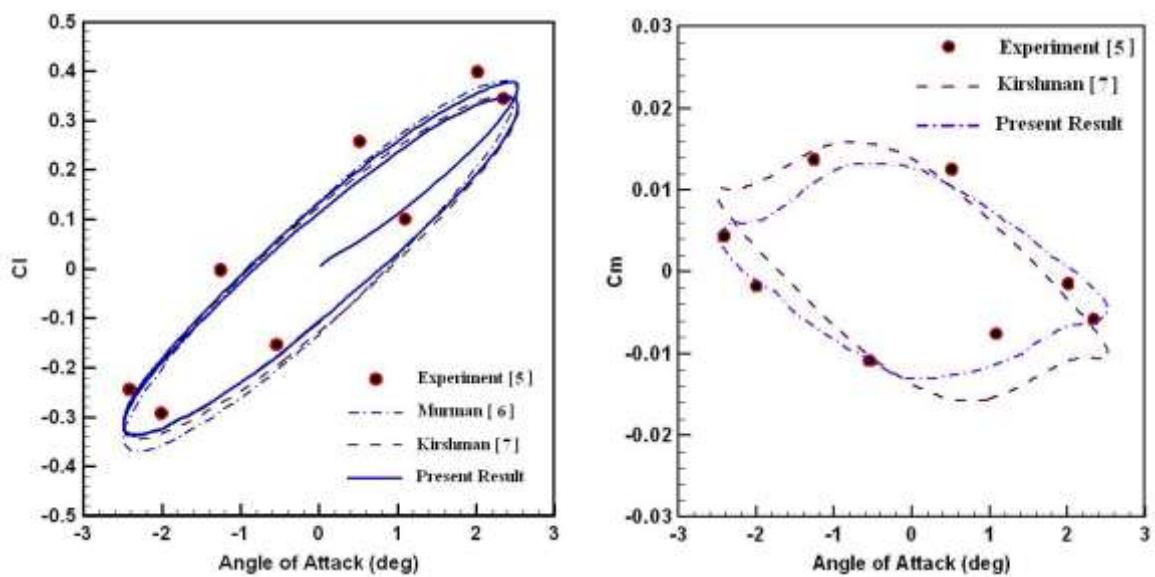


Figure 8. Lift and moment coefficient loops for AGARD test case CT5.